Environmental Science and Pollution Research (2019) 26:33260–33268
https://doi.org/10.1007/s11356-019-06337-x

RESEARCH ARTICLE

Effect of ionic liquid [MIm]HSO_4 on WPCB metal-enriched scraps refined by slurry electrolysis

Yaping Qi[1] · Xiaoxia Yi[1] · Yugai Zhang[1] · Fansong Meng[1] · Jiancheng Shu[1] · Furong Xiu[2] · Zhi Sun[3] · Shuhui Sun[4] · Mengjun Chen[1]

Received: 4 July 2019 / Accepted: 26 August 2019 / Published online: 13 September 2019

Abstract

Waste printed circuit boards (WPCBs) are usually dismantled, crushed, and sorted to WPCB metal-enriched scraps, still containing an amount of non-metallic materials. This research used slurry electrolysis to refine these WPCB metal-enriched scraps and to examine if a standard ionic liquid, [MIm]HSO_4, can replace H_2SO_4 in the system. The impact of the refinement process on metal migration and transformation is discussed in detail. The results demonstrated that metals in WPCB metal-enriched scraps could be successfully refined using slurry electrolysis, and [MIm]HSO_4 can be used to replace H_2SO_4 in the system. When 80% of H_2SO_4 was replaced by [MIm]HSO_4 (electrolyte of 200 mL, 30 g/L $CuSO_4{\cdot}5H_2O$, 60 g/L NaCl, 130 g/L H_2SO_4, and 1.624 A for 4 h), the total metal recovery rate is 85%, and the purity, current efficiency, and particle size of cathode metal powder were 89%, 52%, and 3.77 μm, respectively. Moreover, the microstructure of the cathode metal powder was dendritic in the H_2SO_4-$CuSO_4$-NaCl slurry electrolysis system, whereas at an 80% [MIm]HSO_4 substitution rate slurry electrolysis system, the cathode metal powder was irregular and accumulated as small-sized spherical particles. Thus, replacing inorganic leaching solvents with ionic liquids may provide a potential choice for the resources in WPCB metal-enriched scraps.

Keywords WPCBs · Ionic liquid · Slurry electrolysis · Metals and nonmetals · Refining

Introduction

With progress in information and communication technology, the lifespan of electronic products is becoming shorter and shorter, resulting in a large amount of electronic waste (e-waste) (Abdelbasir et al. 2018; Debnath et al. 2018). The amount of e-waste in the world in 2016 was approximately 44.7 million tons, and it is expected to reach 52.2 million tons in 2021 (Baldé et al. 2017). Printed circuit boards are the basic component of majority of electric and electronic products. Research shows that waste printed circuit boards (WPCBs) account for about 6% weight of e-waste (Zhou and Xu 2012). WPCBs are mainly rich in precious metals and valuable metal, such as gold, palladium, silver, copper, lead, and tin (Imre-Lucaci et al. 2017). For example, in a typical WPCBs, copper, silver, gold, and palladium account for about 16%, 0.05%, 0.03%, and 0.01% weight, respectively, which is far higher than its corresponding metal content in their ordinary ores (Flandinet et al. 2012). Thus, WPCBs can be seen as a rich "urban mine" (Tanskanen 2013). In addition, wide public attention has been attracted because WPCBs contain a large amount of toxic substances, such as brominated flame retardants and heavy metals (Garlapati 2016). If these are not handled properly, they can be a serious threat to the environment and public health (Ghosh et al. 2015). Hence, WPCB recycling—with consideration of ecosystem protection, human health, and the acute shortage of natural minerals globally—is of great significance. At present, most recycling enterprises mainly use dismantling, crushing, and sorting to recycle WPCBs. The resulting product is mainly WPCB metal-enriched scrap which still contains a certain amount of non-metallic materials. Studies

Responsible editor: Bingcai Pan

✉ Mengjun Chen
kyling@swust.edu.cn

[1] Key Laboratory of Solid Waste Treatment and Resource Recycle, Ministry of Education, Southwest University of Science and Technology, Mianyang 621010, China

[2] College of Geology & Environmental, Xi'an University of Science and Technology, Xi'an 710054, China

[3] Institute of Process Engineering, Chinese Academy of Sciences, Beijing 100190, China

[4] Institute National de la Recherché Scientifique-Énergie, Matériaux et Télécommunications, Varennes, QC J3X 1S2, Canada

on WPCB reutilization, including physical-mechanical process (Pinho et al. 2018; Yousef et al. 2017), pyro-metallurgy (Shokri et al. 2017; Weeden et al. 2015; Wang et al. 2017a, b), bio-metallurgy (Faraji et al. 2018; Yin et al. 2018; Yuan et al. 2018), and hydrometallurgy (Batnasan et al. 2018; Haccuria et al. 2017; Kumari et al. 2016; Liu et al. 2017; Popescu et al. 2016), generally use the baseboards as raw material. In contrast, few studies have focused on these WPCB metal-enriched scraps.

Previously, Chu et al. (2015) pressed these WPCB metal-enriched scraps into thick plates, and used them as the anode and electrolyzed directly. The results showed that this process could successfully recover copper from WPCB metal-enriched scraps with a copper purity of 98.1%. More recently, slurry electrolysis, which combines leaching, purification, and electro-deposition in a single step in a tank, characterizing of low reagent use, high efficiency, and low energy consumption (Wu et al. 2017), could be successfully applied to recover high purity superfine copper powders from WPCB metal-enriched scraps with a copper purity of 99.3% (Zhang et al. 2017). During the slurry processing, metals in the anode region undergo an oxidative leaching reaction, and then the metal ions enter the cathode region through the diaphragm, and the metal ions are precipitated after being reduced in the cathode (Yang et al. 2018; Zhang et al. 2019). In addition, Huang et al. (2014) found that ionic liquid, known as a green solution because of specific characteristics, such as good physicochemical stability, weak volatility, good selectivity, high electrochemical stability, and wide chemical window (Chang et al. 2017; Xiao et al. 2018), could be used to leach copper from WPCBs, and the results found that ionic liquid showed a stronger acidity than ordinary inorganic acids with a leaching rate of approximately 100% under the optimum conditions. However, research on acidic ionic liquids in slurry electrolysis for WPCB recycling is limited (Chen et al. 2015; Zhang et al. 2018; Zhu et al. 2012), not to mention WPCB metal-enriched scraps.

The current study aims to assess if the metals in WPCB metal-enriched scraps can be refined and to examine if a typical ionic liquid, [MIm]HSO_4, can replace H_2SO_4 in the slurry electrolysis process. The paper discusses the effect of [MIm]HSO_4 on metal migration and transformation based on the characteristics of metal recovery, metal distribution, purity, current efficiency, phase compositions, and microstructures of the metal powders obtained.

Materials and methods

Sample preparation

The WPCB metal-enriched scraps used in the experiment were provided by a qualified electronic waste recycling enterprise in China. To begin with, these WPCB metal-enriched scraps were dried at 70 °C for 24 h, followed by microwave digestion using a HNO_3-H_2O_2-HF system (Güngör and Elik 2007) and then analyzed by an Inductively Coupled Plasma Optical Emission Spectrometer (ICP-OES, Thermo Scientific, ICAP 6500, MA, USA). Table 1 shows that copper (Cu) was the main metal which accounted for 71.96% weight. The product also contained small amounts of lead (Pb), iron (Fe), aluminum (Al), barium (Ba), zinc (Zn), magnesium (Mg), tin (Sn), and nickel (Ni). The WPCB metal-enriched scrap specimens were further characterized by X-ray diffraction (XRD; D/MAX2500; Rigaku, Almelo, Holland), as shown in Fig. 1. The main components are Cu, followed by Al, Pb, and Sn, which are consistent with the results of digestion.

Slurry electrolysis

The ionic liquid [MIm]HSO_4 is analytical grade and is supplied by a research institute in China. Slurry electrolysis reactor is a rectangular container, made of polytetrafluoroethylene (PTFE). A ruthenium-plated titanium plate was used as the anode and a copper plate was used as the cathode. The electrolyte consisted of 30 g/L $CuSO_4{\cdot}5H_2O$, 60 g/L NaCl, and 130 g/L H_2SO_4, with a volume of 200 mL. WPCB metal-enriched scraps (6 g) were added into the anode chamber, and ozone (3S–A10, Tonglin Technology, Beijing, China) was introduced to the anode chamber at a rate of 1.5 L/min, mechanical stirring at a rate of 300 r/min. The actual area of the plate was 0.02 m^2 and the distance between the plates was 0.095 m. The current value was set to 1.624 A (the current density is 80 mA/cm^2), and the electrolysis time was 4 h. The substitution rate of H_2SO_4 by ionic liquid [MIm]HSO_4 was 0%, 10%, 20%, 40%, 60%, and 80% (v/v).

Characterization

After each run, the cathode and anode plates were taken out. The metal powders in the cathode chamber, residues of WPCB metal-enriched scraps in the anode chamber, and the electrolyte were collected. The cathode metal powder and anode residues were dried at 50 °C for 24 h after passivation with a benzotriazole solution (5 g/L) for preventing oxidation, washing with ethyl alcohol (30% v/v), ultrasound washing for removing foreign ions. The volume of the electrolyte was also measured. Then, the composition of cathode metal powder and anode residues was determined by microwave digestion using the HNO_3-H_2O_2-HF system. Finally, the metal contents in the digestion solution and the residual electrolyte were measured by ICP-OES; the cathode metal powders were

Table 1 Metal contents of the WPCB metal-enriched scrap specimen

Elements	Cu	Pb	Fe	Al	Zn	Mg	Sn	Ni
Contents (wt%)	71.96	2.92	2.43	1.22	0.21	0.14	0.07	0.06

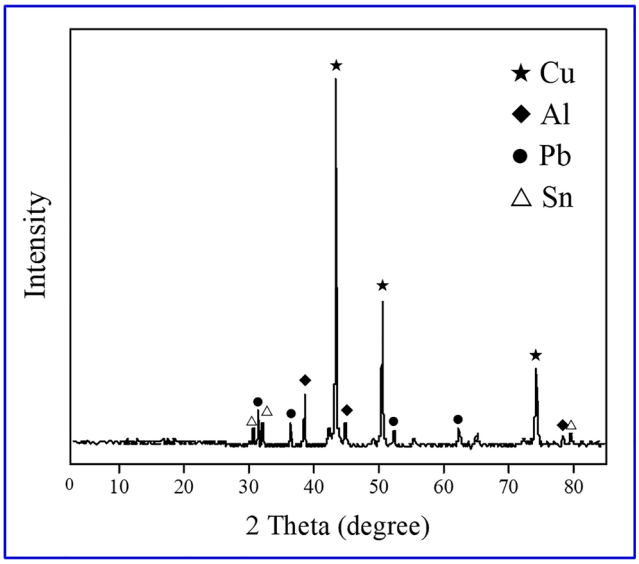

Fig. 1 XRD spectrum of WPCB metal-enriched scrap specimen

further analyzed by XRD, scanning electron microscopy (SEM, Karl Zeiss, EV081A, Heidenheim, Germany), transmission electron microscope (TEM, Carl Zeiss, Libra 200FE, Heidenheim, Germany), and a laser particle size analyzer (LPAS, Bi-90PUS, New York, USA).

The recovery rate of copper (S_{Cu}), the recovery rate of other metals (other than copper) (S_i), the recovery rate of total metals (S_T), current efficiency (η_{Cu}), and purity (P_{Cu}) were calculated as follows:

$$S_{Cu} = \frac{M_y + M_L - M_A}{M_S} \quad (1)$$

where M_y is the mass of copper in the cathode metal powder (g); M_L is the mass of copper in electrolyte (g); M_A is the mass of copper in $CuSO_4{\cdot}5H_2O$ (g); M_S is the mass of copper contained in WPCB metal-enriched scraps (g).

$$S_i = \frac{M_X + M_N}{M_C} \quad (2)$$

where M_x is the mass of the metal (other than copper) in the cathode metal powder (g); M_N is the mass of metal (other than copper) in electrolyte (g); M_C is the mass of metal (other than copper) contained in WPCB metal-enriched scraps (g).

$$S_T = \frac{M_{O+}M_E}{M_z} \quad (3)$$

where M_O is the mass of total metal in the cathode metal powder (g); M_E is the mass of total metal in the electrolyte (g); M_z is the mass of total metal contained in WPCB metal-enriched scraps (g);

$$P_{Cu} = \frac{M_y}{M_O} \quad (4)$$

$$\eta_{Cu} = \frac{M_y}{M_T} \quad (5)$$

where M_T is the theoretical mass of copper obtained by cathode electrolysis based on Faraday's rule as follows:

$$M_T = \frac{M_{Cu}Q}{Z_{Cu}F} \quad (6)$$

where M_{Cu} is molecular mass of copper (63.54 g/mol); Q is electricity, which is the product of current I (A) and electrolytic time T (s); Z_{Cu} is the chemical valence of metals and F is Faraday's constant (96,485.3 C/mol); thus, M_T is a constant value, 7.70.

Results and discussion

Metal recovery

Figure 2 presents the effect of $[MIm]HSO_4$ substitution rate on the recovery rate of Cu, Fe, Al, Mg, Ni, Pb, Sn, Zn, and the total metals. The recovery rate of Cu, Mg, Ni, and Pb decreases as the $[MIm]HSO_4$ substitution rate increases. For example, Cu, Mg, Ni, and Pb recovery rate decreased from 93%, 52%, 99%, and 87% to 82%, 32%, 61%, and 51% respectively when $[MIm]HSO_4$ substitution rate increased from 0 to 80%, indicating an obvious negative relationship. The recovery rate of Al, Fe, Sn, and Zn varied as the $[MIm]HSO_4$ substitution rate increased. A possible reason for this phenomenon could be the selectivity of ionic liquid $[MIm]HSO_4$ to different metals (Wang 2017). In addition, the recovery rate of total metals decreased as the $[MIm]HSO_4$ substitution rate increased showing a similar trend to copper which is the dominant component of total metals. When no H_2SO_4 was substituted by $[MIm]HSO_4$, the recovery rate of total metals was 94%; when the substitution rate of H_2SO_4 by $[MIm]HSO_4$ was 80%, the total metal recovery rate declined to 85%. The reason for this relationship might be the high viscosity of $[MIm]HSO_4$, which may greatly increase the mass transfer resistance in the electrolysis process, thus reducing the recovery rate of total metals (Zhang et al. 2009).

Figure 2 also suggests that the recovery rate of Mg and Al is relatively low, generally lower than 50%, while the recovery rate of other metals—Cu, Fe, Ni, Sn, Pb, and Zn—is much higher, up to 95%. This may be ascribed to their electrode potentials. If the electrode potential of a metal is low, the metal will be easily leached out into the solution, while it is hard to deposit on the cathode. According to the Nernst equation (Eq. (7)), the electrode potential of a metal is mainly dependent on the standard

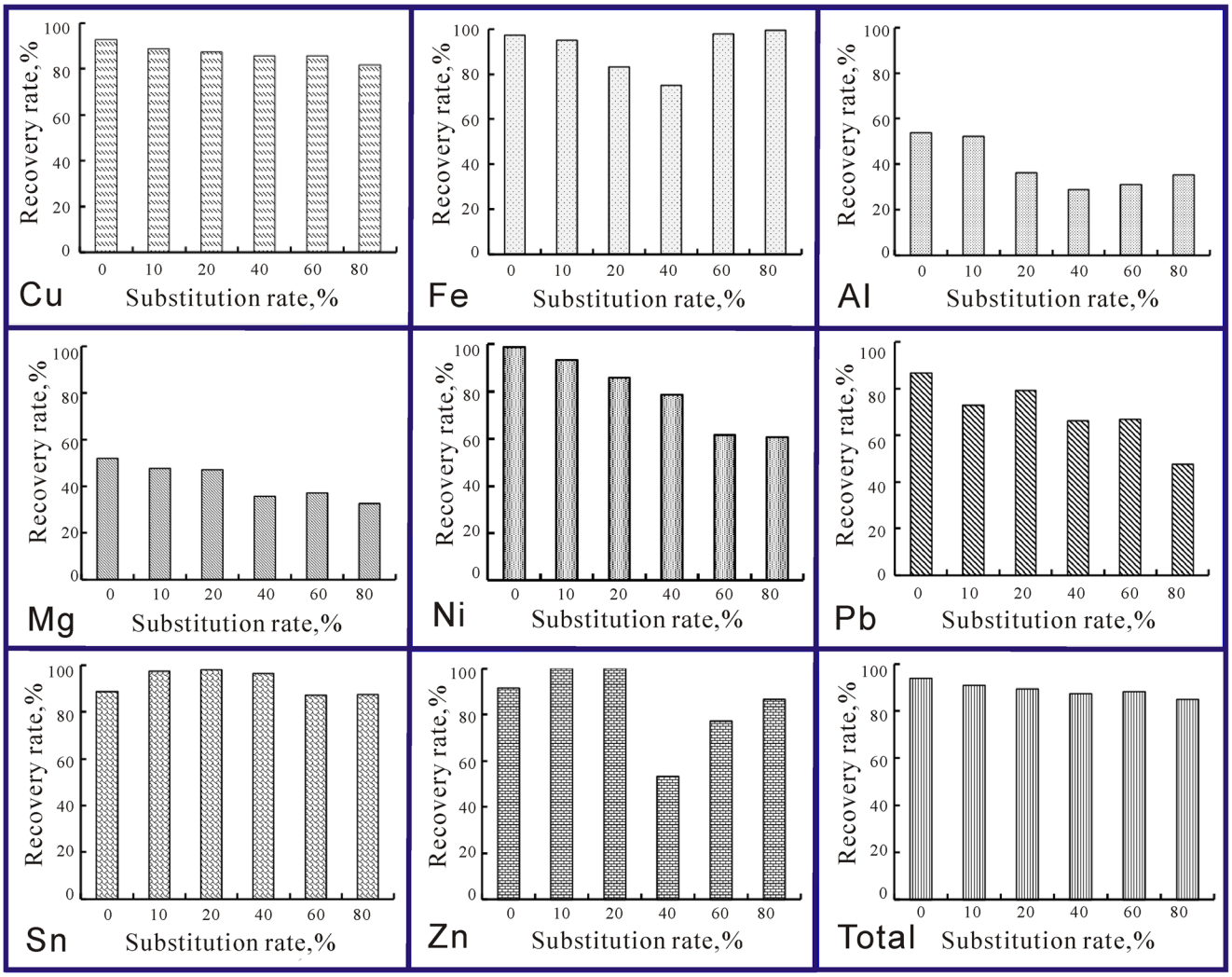

Fig. 2 Effect of $[MIm]HSO_4$ substitution rate on metal recovery

electrode potential and the activity of the metal ions in the solution.

$$E = E^0 + \left(\frac{RT}{nF}\right)\ln a_{M^{Z+}} \quad (7)$$

where E^0 is the standard electrode potential (V); R is gas constant (8.3144 J/(K mol)); T is thermodynamic temperature (K); n is the number of electrons transferred in the electrode reaction; a_M is the activity of metal ions in solution; Z is the valence state of metal ions; and F is Faraday constant (96,485.3 C/mol).

The standard electrode potential of the relevant metals is given in Table 2. Among them, Mg and Al had relatively low standard electrode potential (− 2.375 V and − 1.662 V respectively) in comparison to Cu, Fe, Ni, Sn, Pb, and Zn that had relatively high values (+ 0.337 V, − 0.037 V (Fe^{+3}), − 0.440 V (Fe^{+2}), − 0.257 V, − 0.1375 V, − 0.126 V and − 0.763 V respectively), which is consistent with the results of metal recovery discussed above. In addition, the activity of metal ions in solution is related to its content in WPCB metal-enriched scraps. For example, Mg and Al contents in WPCB metal-enriched scraps were relatively low. Therefore, to some extent, these metals are not conducive to recycling from WPCBs.

The distribution of metals

The substitution of H_2SO_4 by $[MIm]HSO_4$ (Fig. 2) shows some impact on metal recovery, and it significantly affects their distribution in the cathode metal powder, anode residues, and electrolyte.

Figure 3a and b show that the mass contribution of metals when $[MIm]HSO_4$ substitution rate in the slurry electrolysis is 0% and 80%, respectively. The figures indicate that the mass contribution of Cu and Pb in cathode metal powder at 80% substitution rates is lower than those at no substitution, especially for Pb with mass contribution of 83% compared to 52%. This indicates that $[MIm]HSO_4$ could inhibit the deposition of Cu and Pb on the cathode which would further inhibit their

Table 2 Standard electrode potentials for some selected reactions (298.15 K, 101.325 KPa, $a_{M^{z+}}$ =1)

Electrode reactions	Standard electrode potential (V)
$Ba^{2+}+2e^{-}\leftrightarrow Ba$	− 2.900
$Mg^{2+}+2e^{-}\leftrightarrow Mg$	− 2.375
$Al^{3+}+3e^{-}\leftrightarrow Al$	− 1.662
$Zn^{2+}+2e^{-}\leftrightarrow Zn$	− 0.763
$Fe^{2+}+2e^{-}\leftrightarrow Fe$	− 0.440
$Ni^{2+}+2e^{-}\leftrightarrow Ni$	− 0.257
$Sn^{2+}+2e^{-}\leftrightarrow Sn$	− 0.1375
$Pb^{2+}+2e^{-}\leftrightarrow Pb$	− 0.126
$Fe^{3+}+3e^{-}\leftrightarrow Fe$	− 0.037
$2H^{+}+2e^{-}\leftrightarrow H_2$	0
$Cu^{2+}+2e^{-}\leftrightarrow Cu$	+ 0.337
$O_2+4H^{+}+4e^{-}\leftrightarrow 2H_2O$	+ 1.229

Data from CRC Handbook of Chemistry and Physics (97th edition)

separation from WPCB metal-enriched scraps. The mass contribution of Ni in electrolyte shows a similar trend as Cu and Pb (with values of 94% compared to 80% when $[MIm]HSO_4$ substitution rate is 0% and 80%) indicating that $[MIm]HSO_4$ is not conducive to Ni leaching, which inhibits the separation of nickel from WPCB metal-enriched scraps. In contrast to the above, the mass contribution of Al and Mg in anode residue increased from 46 to 58 and 66%, respectively, which is an opposite trend to Cu and Pb, when the substitution rate of $[MIm]HSO_4$ increased from 0 to 80%. This suggests that $[MIm]HSO_4$ is not conducive to the recovery of Al and Mg. Finally, the mass contribution of Sn, Fe, and Zn in the electrolyte is the largest, especially for Fe, with values greater than 95%. Additionally, there is no obvious change in the mass contribution of these three metals in the electrolyte when $[MIm]HSO_4$ substitution rate in the slurry electrolysis is 80%, indicating that $[MIm]HSO_4$ has little effect on the separation of these metals from WPCB metal-enriched scraps.

The above analysis shows that the mass contribution of each metal is different when $[MIm]HSO_4$ substitution rate in the slurry electrolysis is 0% compared to 80%. A potential reason could be that $[MIm]HSO_4$ has certain selectivity for leaching metals in WPCBs, as suggested by Wang et al. (2017a, b). Note that the mass contribution results of the above metals are consistent with the metal recovery explored in Fig. 2. Therefore, it can be concluded that the regular pattern of metal mass contribution is related to its electrode potentials.

Current efficiency, purity, and particle size of cathode metal powder

Figure 4a shows the effect of $[MIm]HSO_4$ substitution rate on cathode metal powder current efficiency and purity, the former decreasing with increase in $[MIm]HSO_4$ substitution rate. For example, current efficiency decreased from 67 to 52% as $[MIm]HSO_4$ substitution rate increased from 0 to 80%, indicating a strong negative relationship. Increase in the substitution rate of $[MIm]HSO_4$ resulted in the purity of cathode metal powder varying around 90%, in the range of 89–93%. A previous study found that the increase of sulfuric acid concentration is favorable to improving the conductivity of the electrolyte, thereby improving its current efficiency (Matsushima et al. 2008). In contrast, our results found that the current efficiency decreased as $[MIm]HSO_4$ substitution rate increased (Fig. 4a). A possible reason for this phenomenon is that the acidity of ionic liquid $[MIm]HSO_4$ is weaker than sulfuric acid, which has been confirmed by previous studies (e.g., Shi et al. 2009). Therefore, the conductivity of the electrolyte is expected to decrease with increase in ionic liquid $[MIm]HSO_4$ substitution rate, leading to a reduction in current efficiency. Moreover, $[MIm]HSO_4$ strongly adsorbs on metal powder surface and increases the mass transfer resistance due to its large molecular mass and viscosity, which is unfavorable

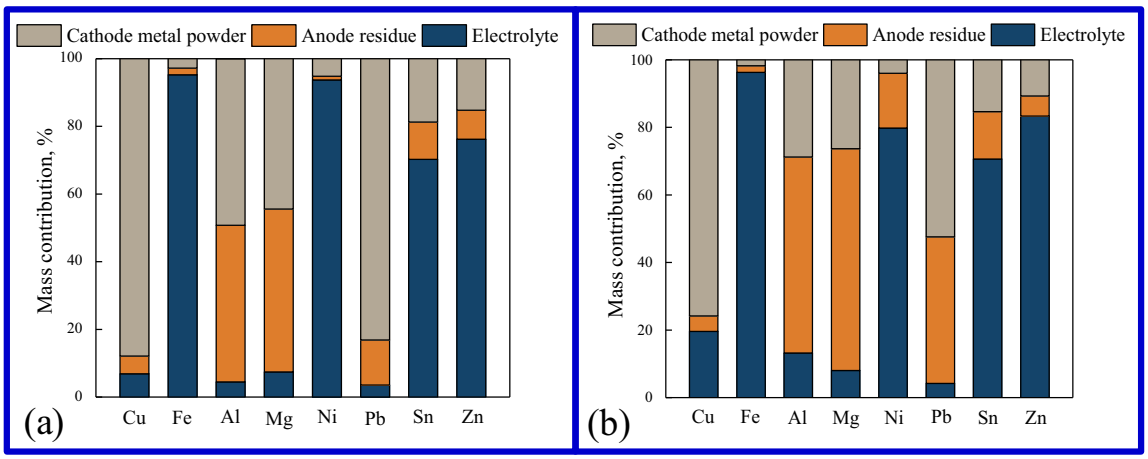

Fig. 3 Metal mass contribution of $[MIm]HSO_4$ substitution rate of 0% and 80%: **a** 0% and **b** 80%

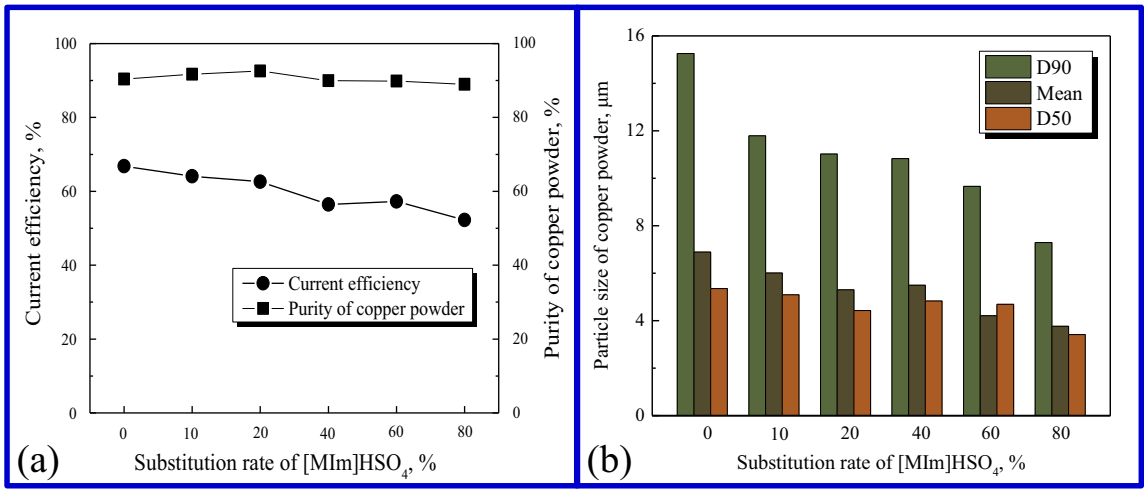

Fig. 4 Effect of $[MIm]HSO_4$ substitution rate on current efficiency, purity, and particle size of cathode metal powder: **a** current efficiency and purity, **b** particle size

to the deposition of copper and improvement of current efficiency (Zhang et al. 2009).

From Eqs. (4) and (5), the following mathematical relationship between P_{Cu}, η_{Cu}, and M_O can be deduced:

$$P_{Cu} = \frac{M_T \times \eta_{Cu}}{M_O} \quad (7)$$

M_T is a constant value, 7.70; M_O is always smaller than the mass of WPCB metal-enriched scraps, 6 g. Thus, the ratio of M_T to M_O is greater than 1. Hence, we can draw the conclusion that the purity of cathode metal powder (P_{Cu}) will always be higher than the current efficiency (η_{Cu}), which is consistent with the results in Fig. 4a. In addition, the purity of cathode metal powder increased slightly and then decreased (Fig. 4a). Meanwhile, there are no other metals that could be detected other than copper. It might be speculated that the cathode metal powder is oxidized by the oxygen in ambient or the slurry electrolysis process, leading to reduction in metal powder purity, and the impurities caused by metal powder oxidation will be further discussed.

Figure 4b shows the effect of $[MIm]HSO_4$ substitution rate on the particle size of cathode metal powder. The mean (average particle size), D50 (50th percentile figure by volume of the particle size distribution), and D90 (90th percentile figure by volume of the particle size distribution) values were used to characterize the particle size of the cathode metal powder. The results found that the particle size of cathode metal powder significantly decreased with increase in the substitution rate of $[MIm]HSO_4$. In the H_2SO_4-$CuSO_4$-NaCl slurry electrolysis system, the mean, D50, and D90 values are 6.89, 5.35, and 15.26 μm, respectively. When the substitution rate is 80%, these three measures declined to 3.77, 3.41, and 7.30 μm, respectively.

Parker (1970) showed that the metal powder obtained by cathode electrolysis is usually crystalline, and its particle size is mainly determined by the ratio of nucleation and crystal growth. When the nucleation rate of the crystal is greater than its growth rate, a large number of nuclei are formed, resulting in smaller particles (Wang et al. 2010). Figure 4b shows that $[MIm]HSO_4$ had a positive effect in reducing the particle size of cathode metal powder. This might be attributed to the ring structure of $[MIm]HSO_4$. Additionally, the –C=N– functional groups reduce the surface tension of the cathode deposited particles and improve the nucleation rate, thus reducing the particle size of the cathode metal powder. However, a previous study (Zhang et al. 2018) that applied $[BSO_3HPy]HSO_4$ to replace sulfuric acid in a slurry electrolytic system for recovering copper from WPCBs found a significant reduction in the average particle size of copper powder from 15.15 to 0.79 μm. This could be because $[BSO_3HPy]HSO_4$ contains not only –C=N– functional groups but also a large π bond, and the hybrid structure formed by the two could reduce the surface tension of the cathode deposited particles more effectively, thus forming smaller metal particles.

Microstructure of the cathode metal powder

The microstructure of cathode metal powder by the H_2SO_4-$CuSO_4$-NaCl slurry system in Fig. 5 (5A, A1, and A2) shows that with $[MIm]HSO_4$ substitution rate of zero, the obtained cathode metal powder was dendritic, which is consistent with our previous research (Zhang et al. 2017, 2018). In contrast, the cathode metal powder is irregular when the substitution rate is 80% and it is aggregated by scattered spherical particles with particle size around 600 nm (Fig. 5 (B, B1 and B2)). The cathode metal powder obtained at the 80% $[MIm]HSO_4$ substitution rate had smaller particle sizes, which is consistent with the results of particle size measurements. A possible reason for this result is that ionic liquid $[MIm]HSO_4$ can form a modified ion layer on the surface of particles, which prevents

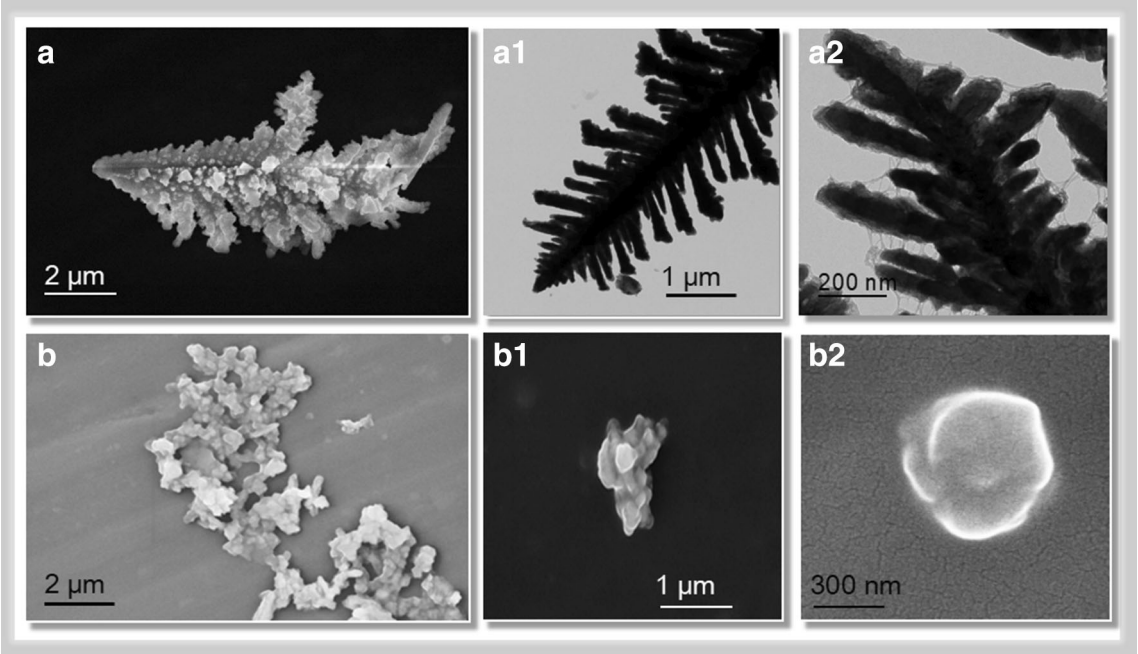

Fig. 5 SEM and TEM results of cathode metal powder in H_2SO_4-$CuSO_4$-NaCl and 80% $[MIm]HSO_4$ substitution rate slurry electrolysis system (image A, B, B1and B2 were obtained by SEM, A1, and A2 by TEM)

the agglomeration of the particles, thereby resulting in smaller metal particles (Yong-Qing et al. 2011). This process thus provides a possibility of controlling the growth of metallic grains in the electrochemical process.

Mineral phase of the cathode metal powder

Figure 6 shows that the phase composition of cathode metal powder was obtained under different $[MIm]HSO_4$ substitution rates of by XRD. Increase in the substitution rate of $[MIm]HSO_4$ results in the phase composition of the cathode metal powder changing slightly. Copper is the main phase in the cathode metal powder as identified by diffraction angles (2θ) of 43.33°, 50.46°, and 74.14°, with the strongest peak at 43.33°. Diffraction angles (2θ) of 36.50°, 42.40°, 61.52°, and 74.14° indicate a phase of Cu_2O. In addition, diffraction angles (2θ) of 29.55°, 36.42°, 42.30°, 61.34°, and 73.53° suggest the existence of $Cu_{2+1}O$. The presence of Cu_2O and $Cu_{2+1}O$

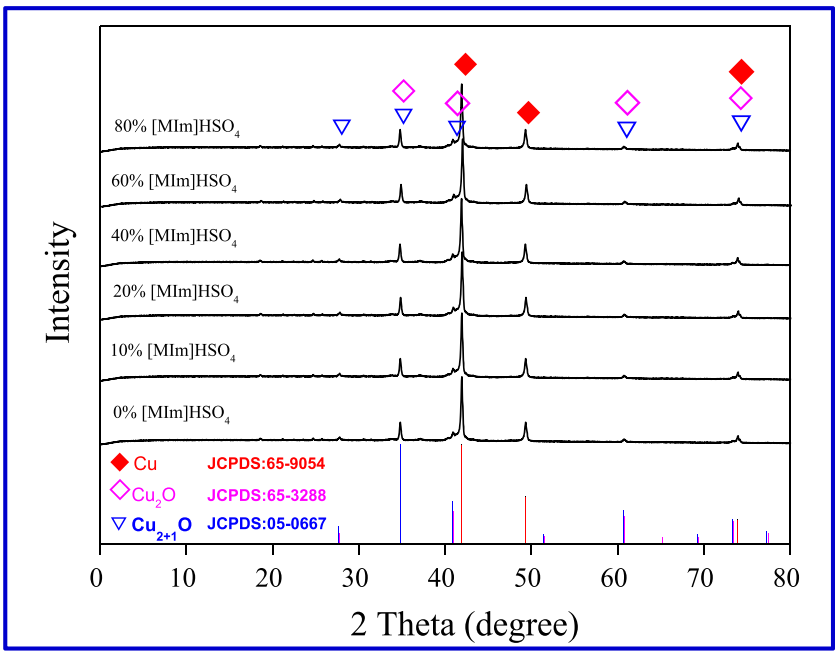

Fig. 6 Mineral phase of cathode metal powder (a–f: $[MIm]HSO_4$ substitution rate of 0, 10, 20, 40, 60, and 80%)

can improve the oxygen content in the sample powders, resulting in reduced copper purity.

Conclusion

In this study, metals in WPCB metal-enriched scraps were refined, and the typical ionic liquid [MIm]HSO_4 was successfully applied to replace H_2SO_4 in the slurry electrolysis system. In addition, the distribution of metals in the cathode metal powder, anode residues, and electrolyte after the slurry electrolysis was significantly affected by the substitution rate of [MIm]HSO_4. The recovery rate of Cu, Mg, Ni, Pb, and total metal decreased as the [MIm]HSO_4 substitution rate increased; in contrast, the recovery rate of Al, Fe, Sn, and Zn varied as [MIm]HSO_4 substitution rate increased. Current efficiency and particle size of cathode metal powder decreased with increase in [MIm]HSO_4 substitution rate, while the purity of cathode metal powder did not change significantly. When 80% of H_2SO_4 was replaced by [MIm]HSO_4 (electrolyte of 200 mL, 30 g/L $CuSO_4{\cdot}5H_2O$, 60 g/L NaCl, 130 g/L H_2SO_4, and 1.624 A for 4 h), the total metal recovery was 85%, and the purity, current efficiency, and particle size of cathode metal powder were 89%, 52%, and 3.77 μm, respectively. Moreover, X-ray diffraction (XRD; D/MAX2500; Rigaku, Almelo, Holland) results showed that [MIm]HSO_4 had negligible effect on the phase composition of cathode metal powder and copper was the main phase, although Cu_2O and $Cu_{2+1}O$ could also be identified. Scanning electron microscopy (SEM, Karl Zeiss, EV081A, Heidenheim, Germany) and transmission electron microscope (TEM, Carl Zeiss, Libra 200FE, Heidenheim, Germany) results indicated that the cathode metal powder was dendritic in structure in a H_2SO_4-$CuSO_4$-NaCl electrolysis slurry system, whereas in an 80% [MIm]HSO_4 substitution rate slurry electrolysis system, the cathode metal powder was irregular and accumulated by small-sized spherical particles. Therefore, replacing inorganic leaching solvents with green ionic liquids cannot only reduce the production of waste acid solution, but also provide a potential choice for the resources in WPCB metal-enriched scraps, which is also providing a theoretical basis for the further industrial application of ionic liquids.

Funding information The research is supported by the National Natural Science Foundation of China (21377104) and Research Fund of Southwest University of Science and Technology (14tdgk01, 17LZX422, 17LZXT05, 18LZX414).

References

Abdelbasir SM, Hassan SSM, Kamel AH, El-Nasr RS (2018) Status of electronic waste recycling techniques: a review. Environ Sci Pollut Res 25:1–15. https://doi.org/10.1007/s11356-018-2136-6

Baldé CP, Forti V, Gray V, Kuehr R, Stegmann P (2017) The global E-waste Monitor-2017, United Nations University (UNU), International Telecommunication Union (ITU) & International Solid Waste Association (ISWA), Bonn/Geneva/Vienna

Batnasan A, Haga K, Shibayama A (2018) Recovery of precious and base metals from waste printed circuit boards using a sequential leaching procedure. JOM 70:124–128. https://doi.org/10.1007/s11837-017-2694-y

Chang GY, Pu Y, Ragauskas AJ (2017) Ionic liquids: promising green solvents for lignocellulosic biomass utilization. Curr Opin Green Sustain Chem 5:5–11. https://doi.org/10.1016/j.cogsc.2017.03.003

Chen MJ, Huang JX, Ogunseitan OA, Zhu NM, Wang YM (2015) Comparative study on copper leaching from waste printed circuit boards by typical ionic liquid acids. Waste Manag 41:142–147. https://doi.org/10.1016/j.wasman.2015.03.037

Chu YY, Chen MJ, Chen S, Wang B, Fu KB, Chen HY (2015) Micro-copper powders recovered from waste printed circuit boards by electrolysis. Hydrometallurgy 156:152–157. https://doi.org/10.1016/j.hydromet.2015.06.006

Debnath B, Chowdhury R, Ghosh SK (2018) Sustainability metal recovery from E-waste. Front Environ Sci Eng 12(2). https://doi.org/10.1007/s11783-018-1044-9

Faraji F, Golmohammadzadeh R, Rashchi F, Alimardani N (2018) Fungal bioleaching of WPCBs using Aspergillus niger: observation, optimization and kinetics. J Environ Manag 217:775–787. https://doi.org/10.1016/j.jenvman.2018.04.043

Flandinet L, Tedjar F, Ghetta V, Fouletier J (2012) Metals recovering from waste printed circuit boards (WPCBs) using molten salts. J Hazard Mater 213:485–490. https://doi.org/10.1016/j.jhazmat.2012.02.037

Garlapati VK (2016) E-waste in India and developed countries: management, recycling, business and biotechnological initiatives. Renew Sustain Energy Rev 54:874–881. https://doi.org/10.1016/j.rser.2015.10.106

Ghosh B, Ghosh MK, Parhi P, Mukherjee PS, Mishra BK (2015) Waste printed circuit boards recycling: an extensive assessment of current status. J Clean Prod 94:5–19. https://doi.org/10.1016/j.jclepro.2015.02.024

Güngör H, Elik A (2007) Comparison of ultrasound-assisted leaching with conventional and acid bomb digestion for determination of metals in sediment samples. Microchem J 86:65–70. https://doi.org/10.1016/j.microc.2006.10.006

Haccuria E, Ning P, Cao H, Venkatesan P, Jin W, Yang Y, Sun Z (2017) Effective treatment for electronic waste - selective recovery of copper by combining electrochemical dissolution and deposition. J Clean Prod 152:150–156. https://doi.org/10.1016/j.jclepro.2017.03.112

Huang JX, Chen MJ, Chen HY, Chen S, Sun Q (2014) Leaching behavior of copper from waste printed circuit boards with Brønsted acidic ionic liquid. Waste Manag 34:483–488. https://doi.org/10.1016/j.wasman.2013.10.027

Imre-Lucaci Á, Nagy M, Imre-Lucaci F, Fogarasi S (2017) Technical and environmental assessment of gold recovery from secondary streams obtained in the processing of waste printed circuit boards. Chem Eng J 309:655–662. https://doi.org/10.1016/j.cej.2016.10.045

Kumari A, Jha MK, Singh RP (2016) Recovery of metals from pyrolyzed PCBs by hydrometallurgical techniques. Hydrometallurgy 165:97–105. https://doi.org/10.1016/6j.hydromet.2015.10.020

Liu XN, Tan QX, Li YG, Xu ZH, Chen MJ (2017) Copper recovery from waste printed circuit boards concentrated metal scraps by electrolysis. Front Environ Sci Eng 11(10.1007/s11783-017-0997-4):10

Matsushima H, Bund A, Plieth W, Kikuchi S, Fukunaka Y (2008) Copper electrodeposition in a magnetic field. Electrochim Acta 53:161–166. https://doi.org/10.1016/j.electacta.2007.01.043

Parker RL (1970) Crystal growth mechanisms: energetics, kinetics, and transport. Solid State Phys 25:151–299. https://doi.org/10.1016/S0081-1947(08)600090

Pinho S, Ferreira M, Almeida MF (2018) A wet dismantling process for the recycling of computer printed circuit boards. Resour Conserv Recycl 132:71–76. https://doi.org/10.1016/j.resconrec.2018.01.022

Popescu AM, Donath C, Neacsu EI, Soare V, Constantin V (2016) Preliminary Study for Copper Recovery in WEEE Leachate by Using Ionic Liquids Based on Choline Chloride. Rev Chim-Bucharest 67:1076–1079. http://www.revistadechimie.ro/pdf/POPESCU%20A

Shi N, Huang BH, Wang YF, Zi-Jin LI, Zhang K, Fang YX (2009) Esterification catalyzed by ionic liquids of imidazolium hydrogen sulfate. Chem Reagents 31:423–426. https://doi.org/10.1016/S1874-8651(10)600798

Shokri A, Pahlevani F, Cole I, Sahajwalla V (2017) Selective thermal transformation of old computer printed circuit boards to Cu-Sn based alloy. J Environ Manag 199:7–12. https://doi.org/10.1016/j.jenvman.2017.05.028

Tanskanen P (2013) Management and recycling of electronic waste. Acta Mater 61:1001–1011. https://doi.org/10.1016/j.actamat.2012.11.005

Wang JQ (2017) Hydrometallurgical leaching technology for WPCBs: the interaction of Cu/Zn/Pb. Southwest University of Science and Technology http://t.cn/Eb4URMu. Accessed 27 March 2017

Wang MY, Wang Z, Guo ZC (2010) Preparation of electrolytic copper powders with high current efficiency enhanced by super gravity field and its mechanism. Trans Nonferrous Metals Soc China 20:1154–1160. https://doi.org/10.1016/s1003-6326(09)60271-5

Wang JQ, Chen MJ, Zhang S, Li FF (2017a) Leaching rule of copper, zinc, lead from waste printed circuit board by ionic liquid. Environ Prot Chem Ind 37:232–236. https://doi.org/10.3969/j.issn.1006-1878.2017.02.019

Wang H, Zhang S, Li B, Pan DA, Wu Y, Zuo T (2017b) Recovery of waste printed circuit boards through pyrometallurgical processing: a review. Resour Conserv Recycl 126:209–218. https://doi.org/10.1016/j.resconrec.2017.08.001

Weeden GS, Soepriatna NH, Nien-Hwa Linda W (2015) Method for efficient recovery of high-purity polycarbonates from electronic waste. Environ Sci Technol 49:2425–2433. https://doi.org/10.1021/es5055786

Wu Z, Yuan W, Li J, Wang X, Liu L, Wang J (2017) A critical review on the recycling of copper and precious metals from waste printed circuit boards using hydrometallurgy. Front Environ Sci Eng 11:31–44. https://doi.org/10.1007/s11783-017-0995-6

Xiao J, Chen G, Li N (2018) Ionic liquid solutions as a green tool for the extraction and isolation of natural products. Molecules 23:1765–1747. https://doi.org/10.3390/molecules23071765

Yang DZ, Chu YY, Wang JB, Chen MJ, Shu JC, Xiu FR, Xu ZH, Sun SH, Chen S (2018) Completely separating metals and nonmetals from waste printed circuit boards by slurry electrolysis. Sep Purif Technol 205:302–307. https://doi.org/10.1016/j.seppur.2018.04.069

Yin S, Wang L, Chen X, Yan R, An K, Zhang L, Wu A (2018) Copper bioleaching in China: review and prospect. Minerals 8:32. https://doi.org/10.3390/min8020032

Yong-Qing SU, Yang MD, Wang YZ, Cong LI, Wang H, Cai Y (2011) Preparation and structure characterization of Ni nanoparticles prepared in medium containing [Bmim]NTf_2 ionic liquids. Nonferrous Metals 3:6–8. https://doi.org/10.3969/j.issn.1007-7545.2011.03.002

Yousef S, Tatariants M, Bendikiene R, Denafas G (2017) Mechanical and thermal characterizations of non-metallic components recycled from waste printed circuit boards. J Clean Prod 167:271–280. https://doi.org/10.1016/j.jclepro.2017.08.195

Yuan Z, Ruan J, Li Y, Qiu R (2018) A new model for simulating microbial cyanide production and optimizing the medium parameters for recovering precious metals from waste printed circuit boards. J Hazard Mater 353:135–141. https://doi.org/10.1016/j.jhazmat.2018.04.007

Zhang QB, Hua YX, Wang YT, Lu HJ, Zhang XY (2009) Effects of ionic liquid additive [BMIM]HSO_4 on copper electro-deposition from acidic sulfate electrolyte. Hydrometallurgy 98:291–297. https://doi.org/10.1016/j.hydromet.2009.05.017

Zhang S, Li YG, Wang R, Xu ZH, Wang B, Chen S, Chen MJ (2017) Superfine copper powders recycled from concentrated metal scraps of waste printed circuit boards by slurry electrolysis. J Clean Prod 152:1–6. https://doi.org/10.1016/j.jclepro.2017.03.087

Zhang YG, Chen MJ, Tan QX, Wang B, Chen S (2018) Recovery of copper from WPCBs using slurry electrolysis with ionic liquid [BSO_3HPy]·HSO_4. Hydrometallurgy 175:150–154. https://doi.org/10.1016/j.hydromet.2017.11.004

Zhang YL, Wang CY, Ma BZ, Jie XW, Xing P (2019) Extracting antimony from high arsenic and gold-containing stibnite ore using slurry electrolysis. Hydrometallurgy 186:284–291. https://doi.org/10.1016/j.hydromet.2019.04.026

Zhou L, Xu Z (2012) Response to waste electrical and electronic equipments in China: legislation, recycling system, and advanced integrated process. Environ Sci Technol 46:4713–4724. https://doi.org/10.1021/es203771m

Zhu P, Chen Y, Wang LY, Qian GY, Zhou M, Zhou J (2012) A new technology for separation and recovery of materials from waste printed circuit boards by dissolving bromine epoxy resins using ionic liquid. J Hazard Mater 239:270–278. https://doi.org/10.1016/j.jhazmat.2012.08.071